

Reactivity of HCO with CH₃ and NH₂ on Water Ice Surfaces. A Comprehensive Accurate Quantum Chemistry Study

Joan Enrique-Romero,^{†,‡} Albert Rimola,^{*,†} Cecilia Ceccarelli,^{*,†} Piero Ugliengo,[¶]
Nadia Balucani,^{§,||,⊥} and Dimitrios Skouteris[#]

[†]*Univ. Grenoble Alpes, Institut de Planétologie et Astrophysique de Grenoble (IPAG),
38000 Grenoble, France*

[‡]*Departament de Química, Universitat Autònoma de Barcelona, 08193, Catalunya, Spain*

[¶]*Dipartimento di Chimica and Nanostructured Interfaces and Surfaces (NIS), Università
degli Studi di Torino, Via P. Giuria 7, 10125 Torino, Italy*

[§]*Dipartimento di Chimica, Biologia e Biotecnologie, Università degli Studi di Perugia, Via
Elce di Sotto 8, I-06123 Perugia, Italy*

^{||}*Osservatorio Astrofisico di Arcetri, Largo E. Fermi 5, 50125 Firenze, Italy*

[⊥]*Univ. Grenoble Alpes, Institut de Planétologie et Astrophysique de Grenoble (IPAG),
38000 Grenoble, France*

[#]*Master-Up, Strada Vicinale Sperandio 15, I-06123 Perugia Italia Perugia, Italy*

E-mail: albert.rimola@uab.cat; cecilia.ceccarelli@univ-grenoble-alpes.fr

Abstract

Interstellar complex organic molecules (iCOMs) can be loosely defined as chemical compounds with at least six atoms in which at least one is carbon. The observations of iCOMs in star-forming regions have shown that they contain an important fraction of

carbon in a molecular form, which can be used to synthesize more complex, even biotic molecules. Hence, iCOMs are major actors in the increasing molecular complexity in space and they might have played a role in the origin of terrestrial life. Understanding how iCOMs are formed is relevant for predicting the ultimate organic chemistry reached in the interstellar medium. One possibility is that they are synthesized on the interstellar grain icy surfaces, via recombination of previously formed radicals. The present work focuses on the reactivity of HCO with CH₃/NH₂ on the grain icy surfaces, investigated by means of quantum chemical simulations. The goal is to carry out a systematic study using different computational approaches and models for the icy surfaces. Specifically, DFT computations have been bench-marked with CASPT2 and CCSD(T) methods, and the ice mantles have been mimicked with cluster models of 1, 2, 18 and 33 H₂O molecules, in which different reaction sites have been considered. Our results indicate that the HCO + CH₃/NH₂ reactions, if they actually occur, have two major competitive channels: the formation of iCOMs CH₃CHO/NH₂CHO, or the formation of CO + CH₄/NH₃. These two channels are either barrierless or present relatively low (≤ 10 kJ/mol equal to about 1200 K) energy barriers. Finally, we briefly discuss the astrophysical implications of these findings.

Keywords

Interstellar medium, Astrochemistry, DFT, iCOMs, grains

1. Introduction

It has been long demonstrated that star forming regions are places with a rich organic chemistry (e.g.¹⁻⁶). Although there are no proofs that organic molecules formed in the interstellar medium (ISM) did play a role in the emergence of terrestrial life, there is mounting evidence that they were inherited by the small objects of the Solar System: for example, carbonaceous chondrites and comets contain a wide variety of organic molecules, some of

them probably being a direct heritage of the ISM based on their relative abundances and ratio of deuterated versus hydrogenated species (e.g.^{4,7-9}).

Knowing how detected interstellar complex organic molecules (iCOMs: C-bearing molecules with at least six atoms¹⁰) are formed and destroyed is not only important per se but also because it is the only way to understand the ultimate organic complexity present in the ISM. Indeed, there is an intrinsic limit to the detection of large iCOMs (excluding linear chains), which is caused by the fact that the larger the molecule the larger the number of rotational transitions (because of the larger number of functional groups of the iCOM) and, consequently, the weaker the intensity of the lines. As a result, the numerous and weak lines of large iCOMs produce a “grass” of lines in the spectra, which makes the identification of a large molecule eventually impossible. Therefore, there is a limit to the largest detectable iCOM, and this has a direct consequence: we need to rely on our knowledge of the processes to predict which large molecules are synthesized in the ISM.

How iCOMs are formed is a question that has baffled astrochemists for decades. In the 90s it was thought that gas-phase reactions were the dominant formation processes (e.g.^{11,12}). However, subsequent astronomical observations (e.g.^{2,13}), laboratory experiments (e.g.¹⁴), and theoretical calculations (e.g.¹⁵) challenged this synthetic route model. As a result, a new paradigm was proposed, which assumes that most (if not all) iCOMs are formed on the surfaces of icy interstellar grains.^{16,17} According to this paradigm, radicals are created by the UV photons impinging on the ice grain mantles, which are formed during the cold cloud/prestellar phase and contain simple hydrogenated species (mostly water but also other species, such as methanol and ammonia, in smaller quantities). With the warming up of the environment caused by the birth of a protostar, the radicals trapped in the ice can diffuse on the grain surfaces and react between them to form iCOMs. The reaction process is assumed to be a direct combination of radicals, which are considered as “lego-like” blocks.

This paradigm is usually assumed in current gas-grain astrochemical models (e.g.¹⁸⁻²²). However, there are still many uncertainties that makes the paradigm not fully validated.

First, it is not clear that the lego-like radical combination is actually an effective process (refs: e.g.^{23,24}). Second, it appears that the role of gas-phase reactions has been underestimated in the past.^{9,25–32} Finally, models based on the “exclusive grain-surface” paradigm are unable to reproduce the observed abundance of several iCOMs (e.g.^{33–35}).

The numerous laboratory experiments reported in the literature are extremely useful to study the possible processes occurring on ices illuminated by UV photons and/or irradiated by energetic particles (e.g.^{36–47}). However, investigating surface-induced iCOMs formation by means of experimental techniques is extremely difficult, if not impossible, since the actual interstellar conditions cannot exactly be reproduced in terrestrial laboratories. For example, the UV irradiation used in laboratory experiments is, for practical reasons, more than million times larger than the one impinging on the interstellar grain mantles: this causes an instantaneous injection of energy of several orders of magnitude larger than that absorbed by the interstellar grain mantles and, consequently, likely introduces different reaction routes (e.g. energy barriers are probably overcome in laboratory experiments while they are not in the cold ISM). Similarly, the H-flux in experiments is also extremely larger compared with the actual ISM conditions, causing a dramatic amplification of the results towards a full saturation of the compounds. A suitable alternative, and certainly a complementary method for such investigations, is the use of theoretical simulations based on quantum chemical calculations. Indeed, these calculations provide a description of the surface reactions from an atomistic perspective, providing unique, relevant energetic information, and, accordingly, they can be useful to assess the validity of the “exclusive grain-surface” paradigm.

In this work, we focus on two reactions occurring on amorphous solid water (ASW) surfaces: $\text{HCO} + \text{CH}_3$ and $\text{HCO} + \text{NH}_2$. In the “exclusive grain-surface” paradigm mentioned above, it is expected that the radical coupling produces two iCOMs: CH_3CHO (acetaldehyde) and NH_2CHO (formamide). However, previous works by some of us^{23,24} showed that other reactive channels can compete with the iCOM formation. Specifically, the two reactions can lead to the formation of $\text{CO} + \text{CH}_4$ and $\text{CO} + \text{NH}_3$, respectively, in which

the H atom of HCO is transferred to the radical partner. Similar processes were identified computationally when HCO reacts with CH₃ on surfaces of CO-pure ices.⁴⁸

The goal of the present work is to carry out a systematic study of two reactions, i.e., HCO + CH₃ and HCO + NH₂, considered here as prototype reactions for the formation of iCOMs, using different approximations for the calculations and models of ASW with the aim to: (1) understand how the different methods and models affect the results, (2) individuate the most convenient methods and models to use in future calculations of other similar radical-radical systems, and (3) identify are the products of the reactions for different conditions. To this end, the present work focuses on the following three points:

1. *Methodology benchmark:* (i) The energy barriers for reactions between the two couples of radicals in the presence of 1 and 2 water molecules are computed with two DFT methods (B3LYP and BHLYP) and compared to the values calculated with the multi-reference CASPT2 method; (ii) The interaction of the three radicals (CH₃, HCO and NH₂) with 1 and 2 water molecules is studied and bench-marked taking as reference the binding energies computed at the CCSD(T) level.
2. *Radical-surface binding enthalpies:* We study the binding of the three radicals (CH₃, HCO and NH₂) to an ASW cluster model of 18 water molecules and to a larger cluster of 33 water molecules sporting two different morphological sites, a cavity and its side.
3. *Radical-radical reactivity:* The reactivity of the two radical couples is studied (i) on the 18 water molecules cluster, and (ii) on the two different morphological sites of the 33 water molecules cluster.

It is worth mentioning that the systems to deal with here sport an additional complexity from an electronic structure point of view. That is, two radicals interacting with water ice, in which the unpaired electrons have opposite signs, constitute a singlet biradical system. Describing this electronic situation with quantum chemistry calculations is delicate. Ab initio multi-reference methods are a good choice to describe biradical systems but they

are extremely expensive and, accordingly, unpractical for large systems. Alternatively, a good compromise between accuracy and computational cost is the DFT broken-symmetry approach.⁴⁹ By using this method, however, our own experience^{23,24} indicates that one has to be sure that the initial guess wave function corresponds to the actual singlet biradical state (i.e., the unpaired electrons being localized on the corresponding radicals and with opposite spin signs), as it may well happen that the initial wave function represents wrongly a closed-shell-like situation, in which the unpaired electrons are 50% distributed among the two radicals. Results derived from one or the other situation are dramatically different.

This article is organized as follows. First the adopted methods are presented (§ 2), then the results are provided following the 3 objectives described above (§ 3) and finally a discussion, including the astrophysical implications, and the conclusions are presented in § 4 and 5, respectively.

2. Methods

All DFT and CCSD(T) calculations were performed using the GAUSSIAN09⁵⁰ software package, while the multi-reference calculations were carried out with the OpenMolcas 18.09^{51–54} program.

Stationary points of the potential energy surfaces (PESs) were fully optimized using two hybrid density functional theory (DFT) methods: B3LYP and BHLYP. These methods have the same Lee, Yang, Parr correlation functional (LYP)⁵⁵ but differ on the exchange functionals: the Becke’s three parameter (B3), which includes a 20% of exact exchange in its definition,⁵⁶ and the Becke’s half-and-half (BH), which mixes the pure DFT and the exact exchange energy in a 1:1 ratio.⁵⁷ For B3LYP calculations, the Grimme’s D3 dispersion term⁵⁸ was accounted for during the geometry optimizations. In contrast, for BHLYP, both the D2⁵⁹ and D3 dispersion terms were included in a posteriori way onto the pure BHLYP optimized geometries.

A calibration study was first carried out for (i) the $\text{NH}_2 + \text{HCO}$ and $\text{CH}_3 + \text{HCO}$ reactivities in the presence of 1 and 2 water molecules (W1 and W2, respectively) and (ii) the interaction of each radical with W1 and W2. For this calibration study, the DFT methods were combined with the Pople's 6-311++G(2df,2pd) basis set. As reference for the reactivity results we used single point energy calculations at the multi-reference CASPT2 level combined with the Dunning's cc-pVTZ basis using as initial guess the orbitals generated at CASSCF(2,2) level. In the same way, single point energy calculations at the CCSD(T)/aug-cc-pVTZ level were also carried out in order to compare them to CASPT2 values. Regarding the interaction energies, the same DFT methods were compared to CCSD(T)/aug-cc-pVTZ level. All the single point energy calculations for this benchmark study were carried out on the B3LYP-D3 optimized geometries.

Radical-radical reactivity was also studied more realistically on two amorphous solid water (ASWs) ices modelled by molecular clusters consisting of 18 (W18) and 33 (W33) water molecules, which were also used in previous works.^{23,24,60} The optimized structures are shown in Figure 1. Interestingly, W33 exhibits a hemispherical cavity and, accordingly, we studied the surface processes considering both this cavity and an extended side of the ice surface (see Figure 1(b)), as they exhibit different surface properties. In order to make the calculations computationally affordable, for these cases the DFT methods were combined with the Pople's 6-31+G(d,p) basis set.

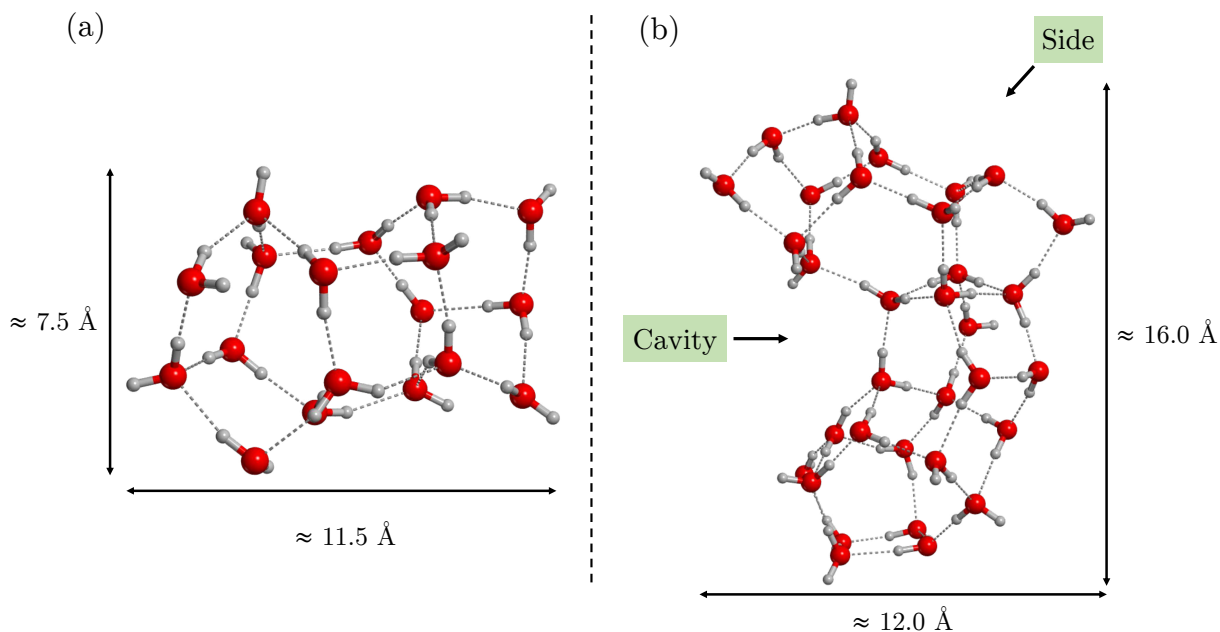


Figure 1: Structures of the 18 and 33 water molecules clusters, (a) and (b) respectively, optimised at the BHLYP/6-31+G(d,p) level.

All stationary points were characterized by the analytical calculation of the harmonic frequencies as minima (reactants, products and intermediates) and saddle points (transition states). Intrinsic reaction coordinate (IRC) calculations at the same level of theory were carried out when needed to ensure that the transition states connect with the corresponding minima. Thermochemical corrections to the potential energy values were carried out using the standard rigid rotor/harmonic oscillator formulas⁶¹ to compute the zero point energy (ZPE) corrections.

Adsorption energies of HCO, CH₃ and NH₂ on W18 and W33 were refined with single point energy calculations combining the DFT methods with the extended 6-311++G(2df,2pd) basis set and corrected for the basis set superposition error (BSSE). Considering *A* as the adsorbate and *B* as the surface cluster model, the BSSE-non-corrected adsorption energy was computed as $\Delta E_{ads} = E_{AB}^{AB}(AB) - E_A^A(A) - E_B^B(B)$, where superscripts denote the basis set used and the subscripts the geometry at which the calculation was done. BSSE-corrected energies were calculated as:

$$\Delta E_{ads}^{CP}(AB) = \Delta E_{ads} + BSSE(A) + BSSE(B) + \delta^A(A) + \delta^B(B) \quad (1)$$

where the BSSE values were calculated following the Boys and Bernardi counterpoise correction method ($BSSE(A) = E_{AB}^{AB}(A) - E_{AB}^A(A)$,⁶²), and where the deformation of each monomer was also accounted for ($\delta^A(A) = E_{AB}^A(A) - E_A^A(A)$).

Inclusion of ZPE corrections allowed us to obtain adsorption enthalpies at 0 K:

$$\Delta H_{ads}(AB) = \Delta E_{ads}^{CP}(AB) + \Delta ZPE \quad (2)$$

In the sign convention followed in this work, the adsorption energy is the negative of the binding energy, i.e. $\Delta E_{ads} = -\Delta E_{bind}$.

The systems containing two radical species were first optimized in the triplet electronic state, which was then optimized in the singlet state to describe the biradical system. Structures with doublet and triplet electronic states were simulated with open-shell calculations based on the unrestricted formalism. Singlet biradicals systems were calculated adopting the unrestricted broken symmetry (BS) approach, in which the most stable initial wave function was found using the *stable=opt* keyword in Gaussian09.

Following the International System Units, all energy units are given in kJ mol^{-1} , whose conversion factor to K is $1 \text{ kJ mol}^{-1} = 120.274 \text{ K}$.

3. Results

In this section, results of the calibration study devoted to the reactivity and interaction of HCO with CH_3 and NH_2 in the presence of 1 and 2 water molecules are first presented. Then, results on adsorption properties and the radical-radical reactions on W18 and W33 are reported.

3.1. Methodology benchmark

This section aims to be a calibration study to check the reliability of the B3LYP and B3LYP methods for (i) the radical-water interactions and (ii) the activation energy of the reactions of CH_3/HCO and NH_2/HCO , in both cases with one and two water molecules (W1 and W2 hereafter) as minimal models representing an ice surface. The references used for the study of the binding and activation energies are CCSD(T) and CASPT2, respectively. In all cases, single point energies were computed onto the B3LYP-D3 optimised geometries. In the supporting information (SI) section the reader can find these geometries as well as the relative errors of the data presented in the following.

Table 1 contains the binding energies for the three radicals involved in this study (namely CH_3 , NH_2 and HCO) interacting with W1 and W2. The systems where a radical interacts with W1 have been based on those presented by Wakelam et al.⁶³, where the initial structures were built in a chemical-wise manner following the ability of each component of the radical to establish a hydrogen bond to a single water molecule, e.g. in the cases where NH_2 and HCO interact with W1 two possibilities were considered: the radicals acting as either H-bond donors (through one of their H atoms), or acting as H-bond acceptors (through the N and O atoms, respectively). The initial geometries of the systems with W2 were built similarly, with the radicals having the maximum number of hydrogen bonds to the two water molecules.

It can be seen that CH_3 is the species having the weakest interaction with the water molecules (6.9-7.1 kJ/mol at the CCSD(T) level). HCO and NH_2 , instead, can form intermediate and strong H-bonds respectively, and, accordingly, they show higher binding energies (11.5-13.2 kJ/mol for the former and 12.8-38.3 kJ/mol for the latter at the CCSD(T) level). This trend is in agreement with that found by Wakelam et al.⁶³, in which the binding energies of these species with W1 were 13, 19-23 and 23-38 kJ/mol for CH_3 , HCO and NH_2 respectively, computed at the M062X/aug-cc-PVTZ level. Note, however, that the quoted values are not the final values used in the model by Wakelam et al.⁶³, as they also use

Table 1: ZPE- and BSSE-non-corrected binding energies computed with different methods for the interaction of CH₃, HCO and NH₂ with 1 and 2 water molecules (W1 and W2) at the B3LYP-D3 and BHLYP levels. None, D2 (accounting for 2-body interactions) and D3 (accounting for 2- and 3-body interactions) dispersion corrections were considered for the latter. BHLYP-based and CCSD(T) values were calculated as single points on the B3LYP-D3 optimised geometries. Energy units are in kJ/mol.

	B3LYP-D3	BHLYP	BHLYP-D2	BHLYP-D3	CCSD(T)
CH ₃ /W1	9.5	5.2	11.3	8.1	6.9
HCO/W1 (H)	12.9	10.9	13.6	13.1	12.0
HCO/W1 (O)	11.7	9.7	12.5	12.1	11.5
NH ₂ /W1 (H)	14.1	12.0	14.9	14.4	12.8
NH ₂ /W1 (N)	23.4	21.5	24.3	23.6	21.6
CH ₃ /W2	8.6	3.1	11.3	8.0	7.1
HCO/W2	14.8	9.2	16.1	15.1	13.2
NH ₂ /W2	41.6	36.6	44.5	41.9	38.3

binding energies from other sources in the literature in order to fit experimental data.

Regarding the performance of the methods, the best ones are B3LYP-D3 and BHLYP-D3, with a relative error of 2-39% and 5-18% respectively (see SI section). The pure BHLYP method systematically underestimates the binding energies, providing strong deviations for CH₃ and HCO, specially on W2. BHLYP-D2 dramatically overestimates the binding energies of CH₃-containing systems (relative errors of $\sim 60\%$), indicating that the D2 term probably accounts for dispersion in excess for this kind of weakly bound complexes.

Table 2 shows the calculated energy barriers of CH₃/HCO and NH₂/HCO on W1 and W2. Three different possible reactions have been identified: i) radical-radical coupling, leading to formation of the iCOMs (i.e. CH₃CHO and NH₂CHO); ii) direct hydrogen abstraction, in which the H atom of HCO is transferred to the other radicals, forming CO + CH₄ and CO + NH₃, respectively; and iii) water assisted hydrogen transfer, the same as ii) but the H transfer is assisted by the water molecules adopting a H relay mechanism. These reactions will be referred to as *Rc*, *dHa* and *wHt*, respectively, along the work.

According to these values, two general trends are observed: (i) *Rc* and *dHa* are either barrierless (meaning that the initial biradical structures were not stable) or have relatively

Table 2: ZPE-non-corrected energy barriers (ΔE^\ddagger), computed with different methods, for radical-radical coupling (Rc), direct hydrogen abstraction (dHa) and water assisted hydrogen transfer (wHt) reactions of $\text{NH}_2 + \text{HCO}$ and $\text{CH}_3 + \text{HCO}$ in the presence of 1 and 2 water molecules computed at the B3LYP-D3 and BHLYP-based levels. For the latter two dispersion corrections have been considered: D2 (which considers all 2-body interactions) and D3 (which considers 2- and 3-body interactions). BHLYP-based, CCSD(T) and CASPT2 values were calculated as single point energy calculations on the B3LYP-D3 optimised geometries. Energy units are in kJ mol^{-1} . NB stands for “No Barrier” and means that the process is found to be barrierless.

System	Process	<i>B3LYP</i> -D3	<i>BHLYP</i>	<i>BHLYP</i> -D2	<i>BHLYP</i> -D3	<i>CCSD(T)</i>	<i>CASPT2</i>
NH_2/HCO ... W1	Rc	NB	NB	NB	NB	NB	NB
	dHa	3.5	6.1	4.1	5.1	5.3	4.2
	wHt	10.9	48.6	46.2	48.8	43.8	48.3
CH_3/HCO ... W1	Rc	NB	NB	NB	NB	NB	NB
	dHa	3.1	6.9	3.3	5.1	5.0	1.5
	wHt	23.5	59.4	55.5	58.6	60.0	52.2
NH_2/HCO ... W2	Rc	6.5	8.5	6.1	6.8	6.3	6.1
	dHa	NB	NB	NB	NB	NB	NB
	wHt	15.5	65.8	62.5	65.1	52.3	52.9
CH_3/HCO ... W2	Rc	NB	NB	NB	NB	NB	NB
	dHa	1.6	4.0	1.5	1.6	1.6	1.0
	wHt	30.7	65.8	62.5	65.1	64.0	52.0

low energy barriers (1.0-6.1 kJ/mol for CASPT2), and (ii) wHt are the processes presenting the highest energy barriers (around 50 kJ/mol for CASPT2).

For those Rc and dHa reactions having an energy barrier, one can see that the worst performance is given by the pure BHLYP method compared to CASPT2. The rest of the methods perform similarly, BHLYP-D2 and B3LYP-D3 being the best ones, which are followed by BHLYP-D3. Regarding the wHt reactions, B3LYP-D3 dramatically underestimates the energy barriers (errors of $\sim 40-80\%$), while BHLYP-based methods perform reasonably well with errors below $\sim 25\%$. CCSD(T) performs similarly to the BHLYP-based methods, presenting moderate energy barrier deviations compared to the CASPT2 values. All errors can be found in the SI section.

In summary, BHLYP-D3 provides the most reliable binding energies, B3LYP-D3, BHLYP-D2 and BHLYP-D3 show good performances for energy barriers related to Rc and dHa processes, while BHLYP-D2 and BHLYP-D3 perform good for wHt energy barriers. Accordingly, and with the aim to be consistent, in the following sections (devoted to the binding and potential energy profiles on the W18 and W33 cluster models) we provide the results at the BHLYP-D3 level of theory, while results based on BHLYP-D2 (on both W18 and W33) and on B3LYP-D3 (on W18) are reported in the SI.

3.2. Radical-surface binding enthalpies

Here we present the ZPE- and BSSE-corrected binding energies of the radicals on the *W18* and *W33* cluster models and their comparison with recent literature. These values are important because binding energies are essential parameters in astrochemical modelling studies.

As it was stated in the previous section, the binding of the radicals on the water ice surfaces are mainly dictated by hydrogen bonds (H-bonds) and dispersion interactions. The clusters exhibit several potential binding sites (Figure 1) and, accordingly, different radical/surface complexes can exist. Here, for the sake of simplicity, we choose those complexes in which the inter-molecular interactions between the two partners are maximized. The

underlying assumption is that radicals on the water ice surfaces have had enough time to thermalize and establish the largest number of inter-molecular interactions with the surface, as very probably is the case in the interstellar conditions. Figure 2 shows the BHLYP-D3 fully optimised complexes on W18 and on the two differentiated W33 sites: its side (W33-side) and its cavity (W33-cav). The corresponding BSSE-corrected binding enthalpies (at 0 K) are also shown. The same information at BHLYP-D2 and B3LYP-D3 is available in SI.

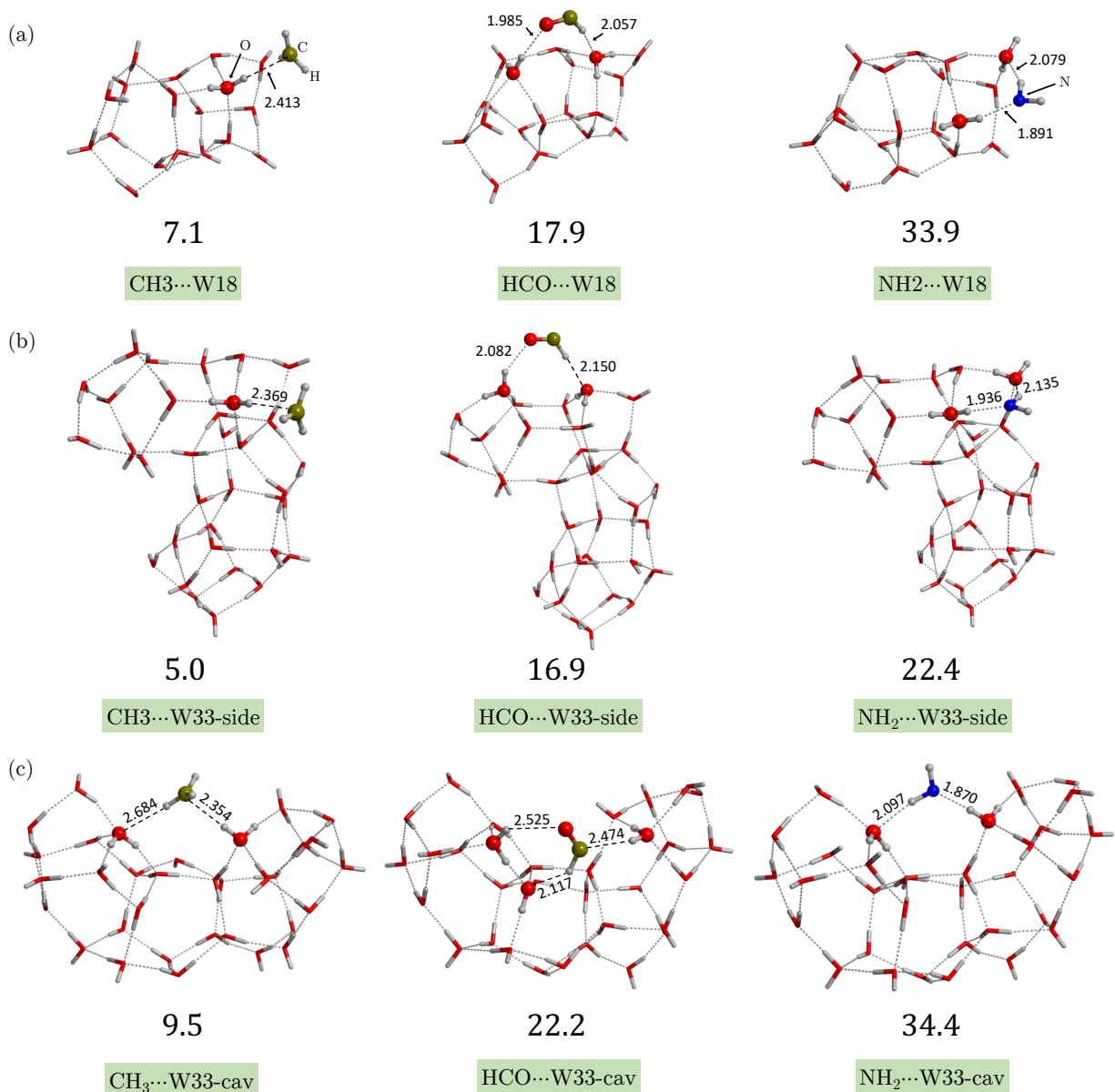


Figure 2: Fully optimized geometries for the binding of CH₃, HCO and NH₂ on (a) W18, (b) W33-side and (c) W33-cav at BHLYP-D3/6-31+G(d,p). Bond distances are in Å. Binding enthalpies (at 0 K) values (in kJ/mol) are corrected for BSSE and are shown below their respective structures.

The binding enthalpy trend is NH₂ > HCO > CH₃, irrespective of the cluster model and surface morphology, in agreement with the results of the previous section. Specifically, the binding enthalpy ranges are: 22.4-34.4, 16.9-22.2 and 5.0-9.5 kJ/mol for NH₂, HCO and CH₃, respectively. These values compare well with those previously computed by Enrique-Romero et al.²⁴ for HCO and CH₃ on the W18 cluster (19 and 6 kJ/mol) and by Rimola

et al.²³ for NH₂ and HCO on the W33-cav cluster (33.5 and 17.5 kJ/mol). In the model presented in Wakelam et al.⁶³, the authors reported binding energies of 27, 20 and 13 kJ/mol for NH₂, HCO and CH₃, respectively, in rough agreement with our results. Sameera et al.⁶⁴ have recently computed the binding energies of HCO and CH₃ adsorbed on hexagonal ice slabs¹. They found HCO binding energies ranging between 12–40 kJ/mol, and 11–25 kJ/mol for HCO and CH₃, respectively. These values are similar or moderately larger than the values found in our W33-cav cluster.

Finally, it is worth mentioning that these complexes do not present hemi-covalent bonds, as it was the case for CN in Rimola et al.²³. Attempts to identify this type of binding in the current systems have been made but the initial structures collapsed to the complexes presented here upon geometry optimization. Therefore, for these systems, the interaction of the radicals with the ice surfaces is essentially dictated by H-bonds and dispersion forces.

3.3. Radical-radical reactivity

In this section, the reactivity of HCO with CH₃ and NH₂ on W18, W33-side and W33-cav are investigated. Given that the chemical environment between W18 and W33-side is similar (note that the surface morphology of W33-side is very similar to that of W18 because W33 was built up by joining two W18 units²³), the comparison of the results between these two models will allow us to assess the effects introduced by the ASW model size. On the other hand, comparison between the reactivity on W33-side and W33-cav will allow us to assess the effects due to different surface environments, namely the presence of a higher number of radical/surface interactions. Please note that the cavity sites are probably more representative of the interstellar conditions than the side sites, as the vast majority of radicals are trapped in the bulk of the ice.

¹Authors used either full DFT with a double- ζ basis set or the ONIOM approach combining DFT with force fields. They reported several values owing to the different adsorption modes of these two species adopting the two computation approaches. This allowed them to report the wide range of binding energies reported here.

Figures 3, 4 and 5 show the PESs of the reactivity of CH_3/HCO and NH_2/HCO calculated at BHLYP-D3 on top of W18, W33-side and W33-cav, respectively. Based on the results for the reactivity in the presence of W1 and W2 (see §3.1), the same three reaction paths, i.e., *Rc*, *dHa* and *wHt*, have been investigated. However, as the later processes are those exhibiting the highest activation enthalpies (as high as 100.6, 78.8, 92.5 and 79.1 kJ/mol for $\text{CH}_3/\text{HCO}\cdots\text{W18}$, $\text{CH}_3/\text{HCO}\cdots\text{W33-cav}$, $\text{NH}_2/\text{HCO}\cdots\text{W18}$ and $\text{NH}_2/\text{HCO}\cdots\text{W33-cav}$, respectively), for the sake of clarity and with the aim of focusing only on the reactions that might play a role in interstellar chemistry, all results related to *wHt* can be found in SI, this section only showing the *Rc* and *dHa* reactions calculated at BHLYP-D3. In the same way, the reader can also find in SI the results for all systems computed at BHLYP-D2 and, for W18, also at B3LYP-D3.

The initial structures of these systems were built according to the interaction patterns present in the single adsorbed radical complexes (see reactant structures of Figures 3-5). The *Rc* and *dHa* reactions, forming acetaldehyde or formamide and $\text{CO}+\text{CH}_4$ or $\text{CO}+\text{NH}_3$, respectively, both take place through a single step. That is, the bond formation between the two radicals for *Rc*, and the H transfer for *dHa*. The only exception is the *dHa* reaction of $\text{CH}_3/\text{HCO}\cdots\text{W18}$, which displays first a submerged activation energy step where HCO breaks its H-bonds with the surface to facilitate the H transfer (see *dHa-TS1* of Figure 3(a)). By comparing the *Rc* and *dHa* reactions on these three cluster models, the general trend is that *Rc* activation enthalpies are lower than the *dHa* ones, between 0.5 - 4 kJ/mol lower. This was already observed in the presence of W1 and W2, where most of the *Rc* reactions are barrierless while the *dHa* present physical (although low) energy barriers. It should be noticed that the HCO/CH_3 reactions on W33-side (Figure 4a) are barrierless due to the ZPE correction, as opposed to the the W1 and W2 cases where the lack of barrier is because of the unstable singlet evolving directly towards products. Indeed, all the stationary points shown in Figure 4(a) have been identified as stable structures in the pure PESs (i.e., without ZPE corrections) but after introduction of ZPE corrections, the transition state becomes lower in

energy than the reactants, and hence the barrierless character.

Another interesting point is that results for W18 and W33-side present some differences, particularly for the $\text{HCO} + \text{CH}_3$ reactions: on W33-side, both Rc and dHa are barrierless while on W18 they present energy barriers. This is indicative of the fact that the size of the cluster for this radical-radical reactivity is important. Finally, no clear trends related to the effect of the ASW ice morphology can be obtained by comparing the W33-side results with the W33-cav. That is, for $\text{HCO} + \text{CH}_3$ reactions, activation enthalpies are higher on W33, while the opposite occurs for $\text{HCO} + \text{NH}_2$ ones.

In the following section, a comprehensive discussion of all these results is provided.

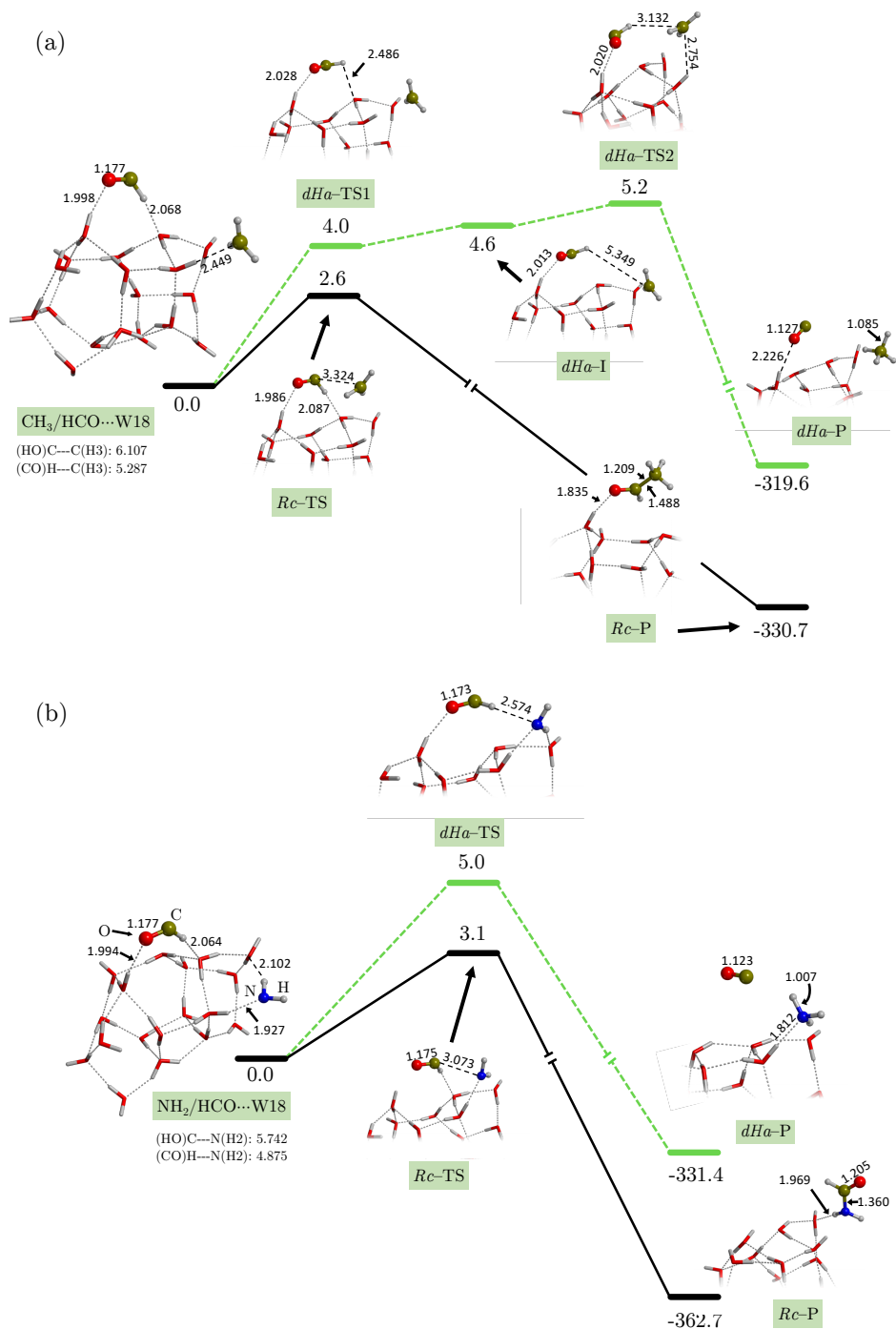


Figure 3: ZPE-corrected Rc (solid black line) and dHa (dashed green lines) PESs for (a) HCO/CH₃...W18 and (b) HCO/NH₂...W18 calculated at the BHLYP-D3/6-31+G(d,p). Energy units are in kJ/mol and distances in Å. Notice that dHa-TS1 for (a) HCO/CH₃...W18 lies below the intermediate dHa-I, due to the ZPE correction, setting effectively a single energy barrier: dHa-Ts2.

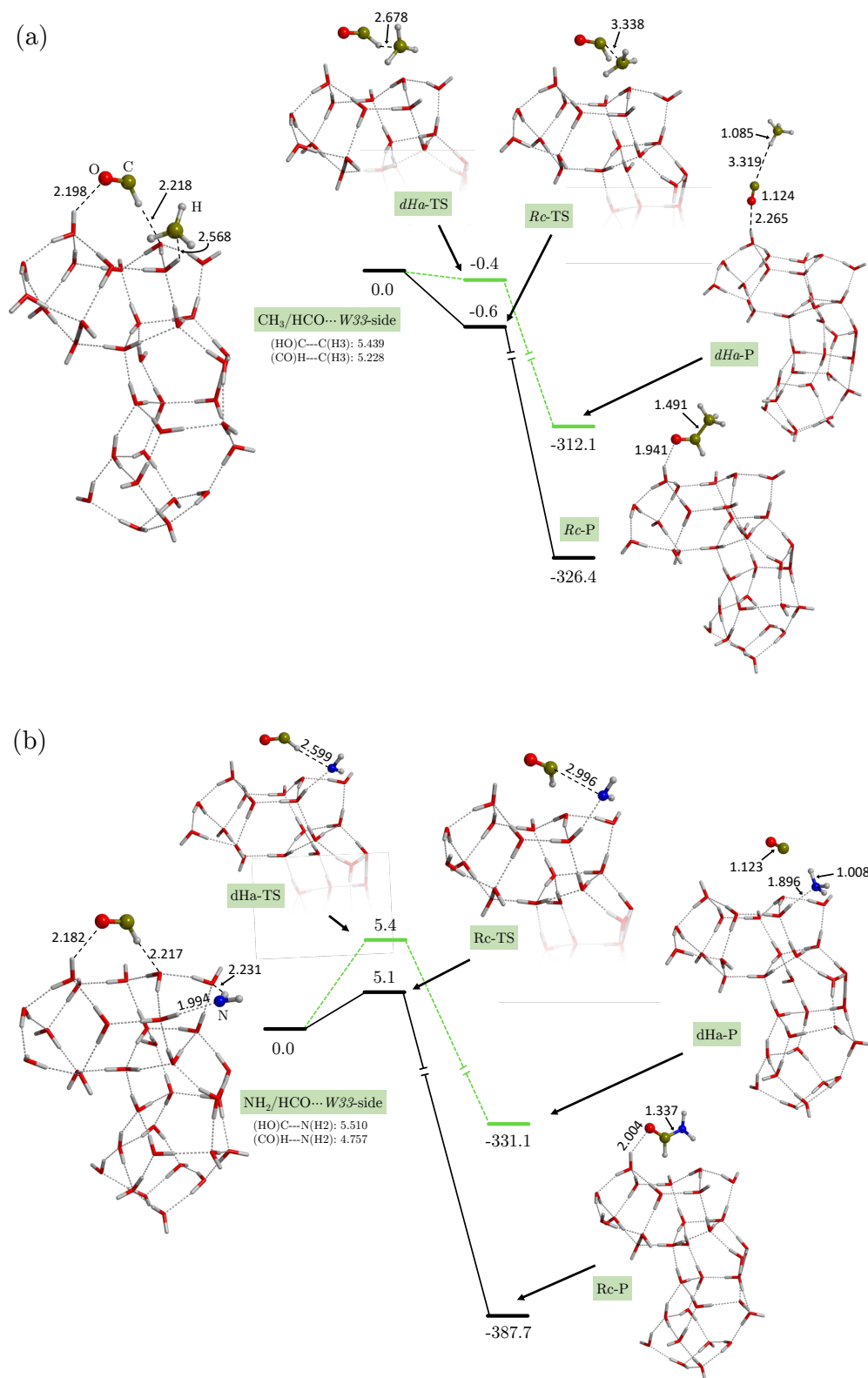


Figure 4: ZPE-corrected Rc (solid black lines) and dHA (green dashed lines) PES for the HCO/CH₃...W33-side (a) and HCO/NH₂...W33-side (b) systems optimized at the BHLYP-D3 theory level. Energy units are in kJ/mol and distances in Å. Notice that both Rc and dHa TS for CH₃/HCO lie below the energy of reactants due to the ZPE correction.

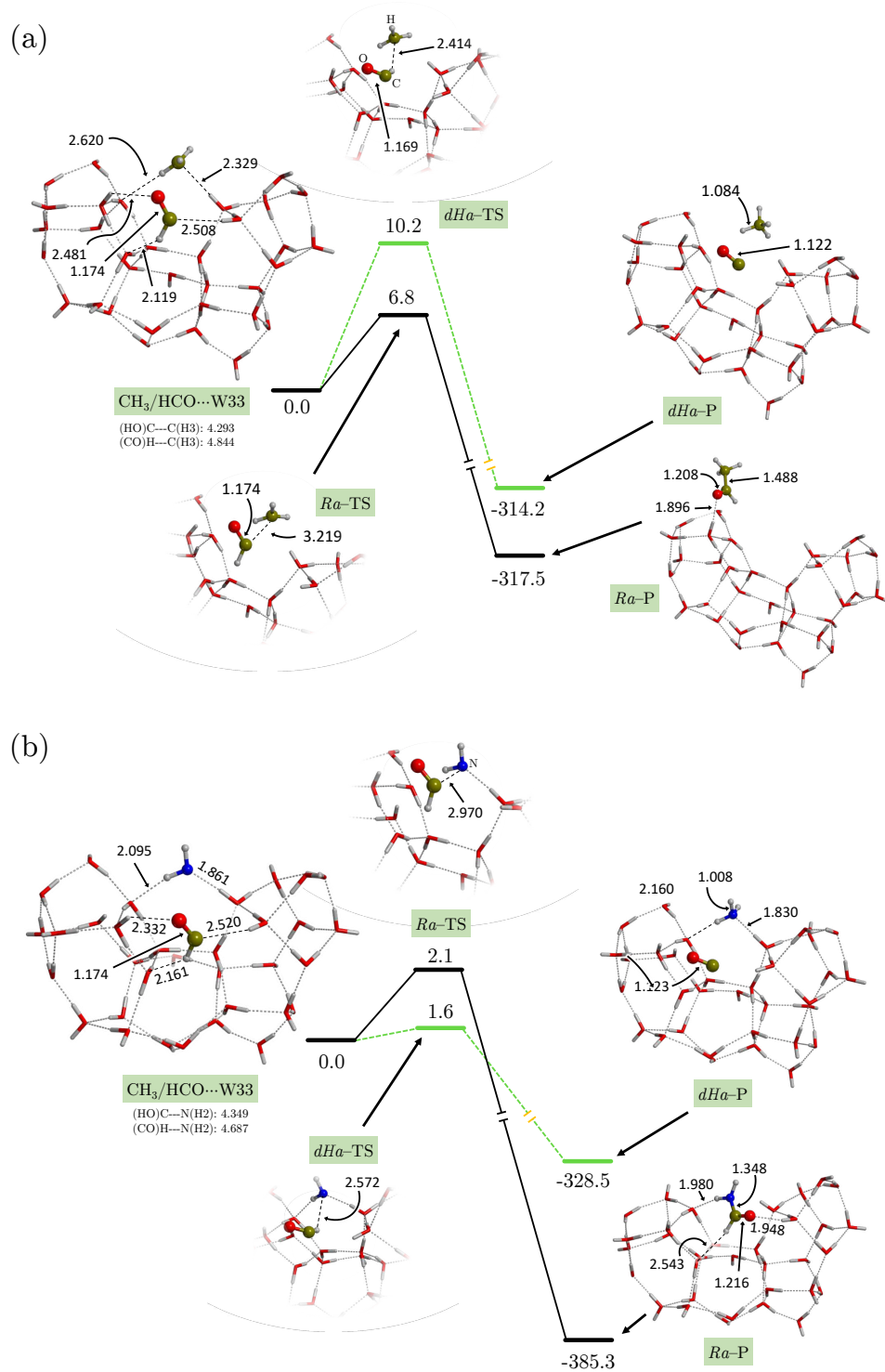


Figure 5: ZPE-corrected Rc (solid black lines) and dHA (green dashed lines) PES for the HCO/CH₃...W33-cav (a) and HCO/NH₂...W33-cav (b) systems optimized at the BHLYP-D3 theory level. Energy units are in kJ/mol and distances in Å. BHLYP-D2 values can be found in the SI.

4. Discussion

4.1 Reaction channels and competition to iCOMs formation

Our computations show that if $\text{HCO} + \text{CH}_3$ and $\text{HCO} + \text{NH}_2$ react on top of an ASW ice, they have two sets of possible reaction products: i) formation of iCOMs (*Rc* process), where the two radical species meet and couple, and ii) the formation of the hydrogenated CH_4/NH_3 species, where the H atom of HCO migrates to CH_3/NH_2 , which can happen either directly (*dHa* process) or through the ice water molecules adopting a H transfer relay mechanism (*wHt* process). The energetics associated with each process at the BHLYP-D3 level are summarised in Table 3.

Table 3: Highest activation enthalpies (at 0 K) for *Rc*, *dHa* and *wHt* reactions on W18, W33-side and W33-cav at the BHLYP-D3 level. Note that NB stands for “No Barrier”. Units are in kJ/mol.

Sys	W18			W33-side			W33-cav		
	Rc	dHa	wHt	Rc	dHa	wHt	Rc	dHa	wHt
$\text{HCO} + \text{CH}_3$	2.6	5.2	100.6	NB	NB	-	6.8	10.2	78.8
$\text{HCO} + \text{NH}_2$	3.1	5.0	92.5	5.1	5.4	-	2.1	1.6	79.1

The *Rc* and *dHa* reactions show, in all the studied systems, similar energetic features, i.e., they are either barrierless or exhibit relatively low energy barriers. The highest pair of energy barriers concerns the $\text{HCO} + \text{CH}_3$ reactions on W33-cav, i.e., 6.8 and 10.2 kJ/mol for *Rc* and *dHa*, respectively. As a general trend, *dHa* reactions have slightly higher activation energies than *Rc* (by as much as 3.4 kJ/mol for HCO/CH_3 and 1.9 kJ/mol for HCO/NH_2). In some cases, like $\text{HCO}/\text{CH}_3 \cdots \text{W33-side}$, $\text{HCO}/\text{NH}_2 \cdots \text{W33-side}$ and $\text{HCO}/\text{NH}_2 \cdots \text{W33-cav}$ both *Rc* and *dHa* can be considered as competitive reactions given the small activation energy differences. In contrast, the lowest energy barriers for *wHt* $\text{HCO} + \text{CH}_3$ and $\text{HCO} + \text{NH}_2$ reactions are ~ 80 kJ/mol, respectively. These values are larger than any *Rc* and *dHa* energy barrier and, accordingly, *wHt* reactions cannot be considered by any means as competitive channels. The explanation of these energetic differences is provided by the re-

action mechanisms. *Rc* and *dHa* reactions take place, in most of the cases, in a concerted way, in which the radicals, in essence, have to partly break the interactions with the surface to proceed with the reaction. In contrast, most of the *wHt* reactions adopt a multi-step mechanism since the H transfer, which is assisted by different ice water molecules, involves different breaking/formation bonds. In these cases, high energy intermediates consisting of the coexistence of HCO and an OH radical are involved (see SI).

In previous works by some of us, (e.g.²⁴) the *wHt* reactions between $\text{CH}_3 + \text{HCO}$ on the W18 cluster model were observed to spontaneously occur during geometry optimisation, i.e. they were found to be barrierless. The difference with the computations presented in this work resides on the fact that, in the previous work,²⁴ the initial wave function did not describe a singlet biradical system but a metastable singlet closed-shell-like one, and hence the spontaneous evolution to form $\text{CO} + \text{CH}_4$. In this work, as well as in Rimola et al. (2018),²³ the initial wave function is actually describing a singlet biradical situation, which leads to a significant stabilization of the reactants and hence the presence of high energy barriers.

Finally, some words related to the chemical role played by the ice on these reactions are here provided. The *Rc* and *dHa* processes in the gas-phase (namely, in the absence of the icy grain) are, in both cases, barrierless. In contrast as explained above, in the presence of the surface, they exhibit, although low, energy barriers. Accordingly, from a rigorous chemical kinetics standpoint, the grains slow down the reactions. This leads us to think that a major role played by the grains is as that of third bodies, by quickly absorbing the nascent energy associated with the reactions, hence stabilising the products. This aspect is particularly appealing in the iCOMs formation processes via radical recombination since in the gas phase iCOMs can redissociate back to reactants if they are not stabilised through three-body reactions. As we will discuss below, the water morphology plays a role in the reaction energetics, although it does not change the essence of our conclusions.

4.2 Influence of the water ice surface model

Clear differences arise when comparing W33-side and W33-cav, as radicals on the latter exhibit more inter-molecular interactions with the surface. This can be seen for example in the binding energies (higher on W33-cav than on W33-side, see Figure 2). But also on the Rc and dHa energy barriers, for which a different behaviour is observed. Indeed, for $\text{HCO} + \text{CH}_3$ these reactions are barrierless on W33-side, while on W33-cav they present energy barriers of 7 (Rc) and 10 (dHa) kJ/mol. On the other hand, for $\text{HCO} + \text{NH}_2$ the opposite behaviour is observed: the energy barriers are higher on W33-side than on W33-cav (see Table 3). This might be indicating that the different polarity of the radicals, i.e., CH_3 /apolar and NH_2 /polar, is important when several polar-based inter-molecular interactions surround the reaction sites, like it is the case of W33-cav.

Finally, the size difference between the W18 and W33 models does not seem to provide a consistent trend, neither for binding energies nor for the PESs. This is probably due to the modest energetics of reactions of interest, which are the result of many intermingled effects, i.e. H-bond and dispersion interaction strength, small charge transfer and polarization. All these components are affected by the nature and size of the water adopted clusters without a definite and predictable structure-properties relationship.

4.3 Astrophysical implications

A major goal of this study is to understand whether iCOMs can be formed on the icy grain surfaces by the direct combination of radicals, a process assumed to be efficient in the majority of current astrochemical models (see Introduction). The present computations show that (i) there is a feasible channel leading to iCOM formation through radical-radical combination, (ii) this channel may possess a barrier, and (iii) there is at least a competitive reaction where radicals exchange a hydrogen atom, the outcome of which is somewhat a step backwards in chemical complexity as the products are simple hydrogenated species (CH_4

and NH_3 in the current work) and CO .

The present computational data does not allow us to definitively exclude the presence of a barrier in the radicals combination. Indeed, although common sense would indicate a lack of barrier, calculations show that the presence of the ice water molecules introduces an inter-molecular interaction that depends on where the radicals are placed and on the radical polarity. This interaction probably necessitates energy to be broken: it is not obvious that this energy is available in the ISM environments. In fact, according to Garrod et al. model,¹⁶ once the radicals are formed, they remain frozen on the ice and subsequently more ice layers build up on top. The radicals remain imprisoned in cavity structures inside the mantle and once the temperature reaches ~ 30 K due to the evolution of the central protostar, they diffuse and react. Among the 3 reactions sites discussed in this article (W18, W33-side and W33-cav), the one best resembling this picture is given by W33-cav (see Figure 1) due to the larger number of inter-molecular interactions. The Rc and dHa energy barriers in the cavity have been shown to be larger for $\text{HCO} + \text{CH}_3$ than for $\text{HCO} + \text{NH}_2$, due probably to the different polarity of CH_3 and NH_2 . If converted to Kelvin, the Rc and dHa barriers for $\text{HCO} + \text{CH}_3$ and $\text{HCO} + \text{NH}_2$ on W33-cav are about 800, 1200, 250 and 190 K, respectively (see Table 3). Thus, the efficiency of these reactions is not expected to be very high, especially for $\text{HCO} + \text{CH}_3$.

It has also to be noted that the starting points from where we study the reactivity in W33-cav (see reactant geometries from Figure 5) contain both radicals very close by and in the same cavity site (given the computational cost of higher quality calculations we cannot simulate much larger clusters). However, in a more realistic situation each radical would be stored in different cavities and thus the actual barriers to overcome would not only involve breaking the radical/ice inter-molecular interactions, but also surmounting the ice surface diffusional barriers, decreasing in this way the efficiency of Rc and dHa reactions, even if they were ultimately barrierless.

We conclude this part mentioning that astronomical observations can also bring useful

constraints to the formation routes of iCOMs showing alternative routes to the ones explored in this study. For example, high spatial resolution observations of formamide line emission towards the protostellar shock site L1157-B1 have demonstrated that the formation of formamide is dominated by the gas-phase reaction $\text{NH}_2 + \text{H}_2\text{CO}$ ⁶⁵, a reaction theoretically studied by some of us.^{66,67} On the same line, observations of the deuterated forms of formamide (namely containing D rather than H atoms) also provide strong constraints on the formation route of this species in the hot corino of the solar-type protostar IRAS 16293-2422. The comparison of the measured $\text{NHDHCO}/\text{NH}_2\text{CHO}$ and $\text{NH}_2\text{CDO}/\text{NH}_2\text{CHO}$ abundance ratios³³ with those predicted by theoretical quantum chemical calculations⁶⁷ strongly favors a gas-phase origin of formamide also in this source. Therefore, it is very likely that both grain-surface and gas-phase reactions contribute to the enrichment of iCOMs in the ISM, playing different roles in different environments.

5. Conclusions and perspectives

In this work, we have carried out an accurate study of the chemistry of two couples of radicals, $\text{HCO} + \text{CH}_3$ and $\text{HCO} + \text{NH}_2$, on icy surfaces. Our goal was to understand the possible reactions between the two radicals on water ice mantles, and how the results depend on the accuracy of the employed quantum chemical methods and on the adopted surface models. To this end, we used different quantum chemistry methods, in particular two hybrid DFT methods, B3LYP and BHLYP, plus the wave function based CCSD(T) and multi reference-based CASPT2 ones. In addition, we adopted different cluster models simulating the water surfaces: we started with the simple cases of one and two water molecules to identify the basic processes and to test the methodology, and then using two different, large molecular cluster models for the ASW surfaces, of 18 and 33 water molecules, respectively.

The conclusions of this work are the following:

1. If the reaction occurs, two channels are possible: (i) the combination of radicals into

acetaldehyde/formamide and (ii) the formation of CH_4/NH_3 plus CO , where the H atom of HCO is passed to CH_3/NH_2 via H abstraction.

2. The two reaction channels are either barrierless or have relatively low energy barriers, from about 2 to 10 kJ/mol, as summarized in Table 3.
3. Comparison of the results obtained with B3LYP-D3 and BHLYP (the latter in its pure definition and including both D2 and D3 dispersion corrections) with those provided by CASPT2 for activation energies and those provided by CCSD(T) for binding energies, using one and two water molecules plus the radicals as test systems, indicates that B3LYP-D3 underestimates the energy barriers, while BHLYP-based methods show a reasonably good performance. For the computations relative to the 18 and 33 water clusters, we adopted BHLYP-D3 as it has been found, in the test systems, to properly deal with both the radical/surface binding and the radical-radical activation energies.
4. The morphology of the water cluster used for the simulations definitely affects the results of the computations. In particular, radicals would interact differently depending on whether they sit on a cavity structure, where they can establish several weak inter-molecular interactions with the icy water molecules, in addition to the H-bond.
5. Taking into account the results described in points 1, 2 and 4, the mechanism that radical combination necessarily produces iCOMs is still to be validated, and should be taken with care in astrochemical models.

In order to make progresses, more accurate computations would be needed, but they are not yet within the reach of the current computational capacities. On the other hand, dynamical simulations would help to understand the effect of the relative orientation of radicals upon encounter.

Supporting information

Structures and errors of the benchmark study, PESs of water assisted H-transfer reactions on W18 and W33-cav, structures, binding energies and PESs (of radical-radical coupling, direct H-abstraction and water assisted H-transfer reactions) on the three analysed surfaces (W18, W33-side and W33-cav) at BHLYP-D2 and on W18 at B3LYP-D3, and optimized Cartesian coordinates of all the structures.

Acknowledgement

JER and CC acknowledge funding from the European Research Council (ERC) under the European Union’s Horizon 2020 research and innovation program, for the Project “the Dawn of Organic Chemistry” (DOC), grant agreement No 741002. AR is indebted to “Ramón y Cajal” program. MINECO (project CTQ2017-89132-P) and DIUE (project 2017SGR1323) are acknowledged. PU and NB acknowledge MIUR (Ministero dell’Istruzione, dell’Università e della Ricerca) and from Scuola Normale Superiore (project PRIN 2015, STARS in the CAOS - Simulation Tools for Astrochemical Reactivity and Spectroscopy in the Cyberinfrastructure for Astrochemical Organic Species, cod. 2015F59J3R). This project has received funding from the European Unions Horizon 2020 research and innovation programme under the Marie Skodowska-Curie grant agreement No 811312.

We thank Prof. Gretobape for fruitful and stimulating discussions.

Most of the calculations presented in this paper were performed using the GRICAD infrastructure (<https://gricad.univ-grenoble-alpes.fr>), which is partly supported by the Equip@Meso project (reference ANR-10-EQPX-29-01) of the programme Investissements d’Avenir supervised by the Agence Nationale pour la Recherche. Additionally this work was granted access to the HPC resources of IDRIS under the allocation 2019-A0060810797 attributed by GENCI (Grand Equipement National de Calcul Intensif).

References

- (1) Rubin, R.; Swenson Jr, G.; Benson, R.; Tigelaar, H.; Flygare, W. Microwave detection of interstellar formamide. *Astrophys. J.* **1971**, *169*, L39.
- (2) Cazaux, S.; Tielens, A.; Ceccarelli, C.; Castets, A.; Wakelam, V.; Caux, E.; Parise, B.; Teyssier, D. The Hot Core around the Low-Mass Protostar IRAS 16293–2422: Scoundrels Rule! *Astrophys. J. Lett.* **2003**, *593*, L51.
- (3) Herbst, E.; Van Dishoeck, E. F. Complex organic interstellar molecules. *Annu. Rev. Astron. Astrophys.* **2009**, *47*, 427–480.
- (4) Caselli, P.; Ceccarelli, C. Our astrochemical heritage. *Astron. Astrophys. Rev.* **2012**, *20*, 56.
- (5) Belloche, A.; Meshcheryakov, A.; Garrod, R.; Ilyushin, V.; Alekseev, E.; Motiyenko, R.; Margulès, L.; Müller, H.; Menten, K. Rotational spectroscopy, tentative interstellar detection, and chemical modeling of N-methylformamide. *Astron. Astrophys.* **2017**, *601*, A49.
- (6) McGuire, B. A. 2018 Census of Interstellar, Circumstellar, Extragalactic, Protoplanetary Disk, and Exoplanetary Molecules. *Astrophys. J. Suppl. Ser.* **2018**, *239*, 17.
- (7) Bockelée-Morvan, D. An overview of comet composition. *Proc. Int. Astron. Union* **2011**, *7*, 261–274.
- (8) Ceccarelli, C.; Caselli, P.; Bockelée-Morvan, D.; Mousis, O.; Pizzarello, S.; Robert, F.; Semenov, D. Deuterium Fractionation: The Ariadne’s Thread from the Precollapse Phase to Meteorites and Comets Today. In *Protostars and Planets VI*, ed. by Beuther, Henrik and Klessen, Ralf S. and Dullemond, Cornelis P. and Henning, Thomas (University of Arizona Press, Tucson), **2014**, pp 859-882. DOI: 10.2458/azu.uapress.9780816531240-ch037.

- (9) Bianchi, E.; Codella, C.; Ceccarelli, C.; Vazart, F.; Bachiller, R.; Balucani, N.; Bouvier, M.; DeSimone, M.; Enrique-Romero, J.; Kahane, C.; Lefloch, B.; López-Sepulcre, A.; Ospina-Zamudio, J.; Podio, L.; Taquet, V. The census of interstellar complex organic molecules in the Class I hot corino of SVS13-A. *Mon. Not. R. Astron. Soc.* **2018**, *483*, 1850–1861.
- (10) Ceccarelli, C. et al. Seeds Of Life In Space (SOLIS): The Organic Composition Diversity at 300–1000 au Scale in Solar-type Star-forming Regions. *Astrophys. J.* **2017**, *850*, 176.
- (11) Charnley, S.; Tielens, A.; Millar, T. On the molecular complexity of the hot cores in Orion A-Grain surface chemistry as ‘The last refuge of the scoundrel’. *Astrophys. J.* **1992**, *399*, L71–L74.
- (12) Caselli, P.; Hasegawa, T.; Herbst, E. Chemical differentiation between star-forming regions-The Orion hot core and compact ridge. *Astrophys. J.* **1993**, *408*, 548–558.
- (13) Ceccarelli, C.; Loinard, L.; Castets, A.; Tielens, A.; Caux, E.; Lefloch, B.; Vastel, C. Extended D₂CO emission: The smoking gun of grain surface-chemistry. *Astron. Astrophys.* **2001**, *372*, 998–1004.
- (14) Geppert, W. D.; Thomas, R. D.; Ehlerding, A.; Hellberg, F.; Österdahl, F.; Hamberg, M.; Semaniak, J.; Zhaunerchyk, V.; Kaminska, M.; Källberg, A.; Paal, A.; Larson, M. Dissociative recombination branching ratios and their influence on interstellar clouds. *J. Phys. Conf. Ser.* **2005**, *4*, 26–31.
- (15) Horn, A.; Møllendal, H.; Sekiguchi, O.; Uggerud, E.; Roberts, H.; Herbst, E.; Viggiano, A.; Fridgen, T. D. The gas-phase formation of methyl formate in hot molecular cores. *Astrophys. J.* **2004**, *611*, 605.
- (16) Garrod, R. T.; Herbst, E. Formation of methyl formate and other organic species in the warm-up phase of hot molecular cores. *Astron. Astrophys.* **2006**, *457*, 927–936.

- (17) Herbst, E. The synthesis of large interstellar molecules. *Int. Rev. Phys. Chem.* **2017**, *36*, 287–331.
- (18) Garrod, R. A new modified-rate approach for gas-grain chemical simulations. *Astron. Astrophys.* **2008**, *491*, 239–251.
- (19) Acharyya, K.; Herbst, E. Molecular Development in the Large Magellanic Cloud. *Astrophys. J.* **2015**, *812*, 142.
- (20) Ruaud, M.; Loison, J.; Hickson, K.; Gratier, P.; Hersant, F.; Wakelam, V. Modelling complex organic molecules in dense regions: Eley–Rideal and complex induced reaction. *Mon. Not. R. Astron. Soc.* **2015**, *447*, 4004–4017.
- (21) Drozdovskaya, M. N.; Walsh, C.; Van Dishoeck, E. F.; Furuya, K.; Marboeuf, U.; Thiabaud, A.; Harsono, D.; Visser, R. Cometary ices in forming protoplanetary disc midplanes. *Mon. Not. R. Astron. Soc.* **2016**, *462*, 977–993.
- (22) Vasyunin, A. I.; Caselli, P.; Dulieu, F.; Jiménez-Serra, I. Formation of complex molecules in prestellar cores: a multilayer approach. *Astrophys. J.* **2017**, *842*, 33.
- (23) Rimola, A.; Skouteris, D.; Balucani, N.; Ceccarelli, C.; Enrique-Romero, J.; Taquet, V.; Ugliengo, P. Can Formamide Be Formed on Interstellar Ice? An Atomistic Perspective. *ACS Earth Space Chem.* **2018**, *2*, 720–734.
- (24) Enrique-Romero, J.; Rimola, A.; Ceccarelli, C.; Balucani, N. The (impossible?) formation of acetaldehyde on the grain surfaces: insights from quantum chemical calculations. *Mon. Not. R. Astron. Soc.* **2016**, *459*, L6–L10.
- (25) Balucani, N.; Ceccarelli, C.; Taquet, V. Formation of complex organic molecules in cold objects: the role of gas-phase reactions. *Mon. Not. R. Astron. Soc.* **2015**, *449*, L16–L20.

- (26) Spezia, R.; Jeanvoine, Y.; Hase, W. L.; Song, K.; Largo, A. Synthesis of Formamide and Related Organic Species in the Interstellar Medium via Chemical Dynamics Simulations. *Astrophys. J.* **2016**, *826*, 107.
- (27) Taquet, V.; Wirström, E. S.; Charnley, S. B. Formation and Recondensation of Complex Organic Molecules during Protostellar Luminosity Outbursts. *Astrophys. J.* **2016**, *821*, 46.
- (28) Suzuki, T.; Ohishi, M.; Hirota, T.; Saito, M.; Majumdar, L.; Wakelam, V. Survey Observations of a Possible Glycine Precursor, Methanimine (CH_2NH). *Astrophys. J.* **2016**, *825*, 79.
- (29) Codella, C., et al. Seeds of Life in Space (SOLIS) - II. Formamide in protostellar shocks: Evidence for gas-phase formation. *Astron. Astrophys.* **2017**, *605*, L3.
- (30) Skouteris, D.; Balucani, N.; Ceccarelli, C.; Faginas Lago, N.; Codella, C.; Falcinelli, S.; Rosi, M. Interstellar dimethyl ether gas-phase formation: a quantum chemistry and kinetics study. *Mon. Not. R. Astron. Soc.* **2018**, *482*, 3567–3575.
- (31) Rosi, M.; Skouteris, D.; Casavecchia, P.; Falcinelli, S.; Ceccarelli, C.; Balucani, N. Formation of Nitrogen-Bearing Organic Molecules in the Reaction $\text{NH} + \text{C}_2\text{H}_5$: A Theoretical Investigation and Main Implications for Prebiotic Chemistry in Space. Computational Science and Its Applications – ICCSA 2018 (Melbourne, Australia). Springer International Publishing: Cham (Switzerland), 2018; pp 773–782.
- (32) Skouteris, D.; Balucani, N.; Ceccarelli, C.; Vazart, F.; Puzzarini, C.; Barone, V.; Codella, C.; Lefloch, B. The Genealogical Tree of Ethanol: Gas-phase Formation of Glycolaldehyde, Acetic Acid, and Formic Acid. *Astrophys. J.* **2018**, *854*, 135.
- (33) Coutens, A. et al. The ALMA-PILS survey: First detections of deuterated formamide and deuterated isocyanic acid in the interstellar medium. *Astron. Astrophys.* **2016**, *590*, L6.

- (34) Müller, H. S. P.; Belloche, A.; Xu, L.-H.; Lees, R. M.; Garrod, R. T.; Walters, A.; van Wijngaarden, J.; Lewen, F.; Schlemmer, S.; Menten, K. M. Exploring molecular complexity with ALMA (EMoCA): Alkanethiols and alkanols in Sagittarius B2(N2). *Astron. Astrophys.* **2016**, *587*, A92.
- (35) Ligterink, N. F. W.; Terwisscha van Scheltinga, J.; Taquet, V.; Jørgensen, J. K.; Cazaux, S.; van Dishoeck, E. F.; Linnartz, H. The formation of peptide-like molecules on interstellar dust grains. *Mon. Not. R. Astron. Soc.* **2018**, *480*, 3628–3643.
- (36) Strazzulla, G.; Palumbo, M. Organics produced by ion irradiation of ices: Some recent results. *Adv. Space Res.* **2001**, *27*, 237 – 243.
- (37) Palumbo, M. E.; Baratta, G. A.; Fulvio, D.; Garozzo, M.; Gomis, O.; Leto, G.; Spinella, F.; Strazzulla, G. Ion irradiation of astrophysical ices. *J. Phys. Conf. Ser.* **2008**, *101*, 012002.
- (38) Woods, P. M.; Slater, B.; Raza, Z.; Viti, S.; Brown, W. A.; Burke, D. J. Glycolaldehyde formation via the dimerization of the formyl radical. *Astrophys. J.* **2013**, *777*, 90.
- (39) Fedoseev, G.; Ioppolo, S.; Zhao, D.; Lamberts, T.; Linnartz, H. Low-temperature surface formation of NH₃ and HNCO: hydrogenation of nitrogen atoms in CO-rich interstellar ice analogues. *Mon. Not. R. Astron. Soc.* **2014**, *446*, 439–448.
- (40) Fedoseev, G.; Cuppen, H. M.; Ioppolo, S.; Lamberts, T.; Linnartz, H. Experimental evidence for glycolaldehyde and ethylene glycol formation by surface hydrogenation of CO molecules under dense molecular cloud conditions. *Mon. Not. R. Astron. Soc.* **2015**, *448*, 1288–1297.
- (41) Linnartz, H.; Ioppolo, S.; Fedoseev, G. Atom addition reactions in interstellar ice analogues. *Int. Rev. Phys. Chem.* **2015**, *34*, 205–237.

- (42) de Barros, A. L. F.; da Silveira, E. F.; Fulvio, D.; Boduch, P.; Rothard, H. Formation of nitrogen- and oxygen-bearing molecules from radiolysis of nitrous oxide ices implications for Solar system and interstellar ices. *Mon. Not. R. Astron. Soc.* **2016**, *465*, 3281–3290.
- (43) Butscher, T.; Duvernay, F.; Rimola, A.; Segado-Centellas, M.; Chiavassa, T. Radical recombination in interstellar ices, a not so simple mechanism. *Phys. Chem. Chem. Phys.* **2017**, *19*, 2857–2866.
- (44) Fedoseev, G.; Chuang, K.-J.; Ioppolo, S.; Qasim, D.; van Dishoeck, E. F.; Linnartz, H. Formation of Glycerol through Hydrogenation of CO Ice under Prestellar Core Conditions. *Astrophys. J.* **2017**, *842*, 52.
- (45) Arumainayagam, C. R.; Garrod, R. T.; Boyer, M. C.; Hay, A. K.; Bao, S. T.; Campbell, J. S.; Wang, J.; Nowak, C. M.; Arumainayagam, M. R.; Hodge, P. J. Extraterrestrial prebiotic molecules: photochemistry vs. radiation chemistry of interstellar ices. *Chem. Soc. Rev.* **2019**, *48*, 2293–2314.
- (46) Dulieu, F.; Nguyen, T.; Congiu, E.; Baouche, S.; Taquet, V. Efficient formation route of the prebiotic molecule formamide on interstellar dust grains. *Mon. Not. R. Astron. Soc.: Letters* **2019**, *484*, L119–L123.
- (47) Pereira, R.; de Barros, A.; Fulvio, D.; Boduch, P.; Rothard, H.; da Silveira, E. NO bearing molecules produced by radiolysis of N₂O and N₂O:CO₂ ices. **2019**, *Nucl. Instrum. Methods Phys. Res., Sect. B*. DOI: 10.1016/j.nimb.2019.03.048.
- (48) Lamberts, T.; Markmeyer, M. N.; Kolb, F. J.; Kstner, J. Formation of Acetaldehyde on CO-Rich Ices. *ACS Earth Space Chem.* **2019**, *3*, 958–963.
- (49) Abe, M. Diradicals. *Chem. Rev.* **2013**, *113*, 7011–7088.

- (50) Frisch, M. J. et al. Gaussian09 Revision D.01. 2009; Gaussian Inc. Wallingford CT 2009.
- (51) Karlström, G.; Lindh, R.; Malmqvist, P.-Å.; Roos, B. O.; Ryde, U.; Veryazov, V.; Widmark, P.-O.; Cossi, M.; Schimmelpfennig, B.; Neogrady, P.; Seijo, L. MOLCAS: a program package for computational chemistry. *Comput. Mater. Sci.* **2003**, *28*, 222 – 239, Proceedings of the Symposium on Software Development for Process and Materials Design.
- (52) Aquilante, Francesco,; De Vico, Luca,; Ferré, Nicolas,; Ghigo, Giovanni,; Malmqvist, Per-åke,; Neogrady, P.; Pedersen, T. B.; Pitoňák, M.; Reiher, M.; Roos, B. O.; Serrano-Andrés, L.; Urban, M.; Veryazov, V.; Lindh, R. MOLCAS 7: The Next Generation. *J. Comput. Chem.* **2010**, *31*, 224–247.
- (53) Aquilante, Francesco, et al. Molcas 8: New capabilities for multiconfigurational quantum chemical calculations across the periodic table. *J. Comput. Chem.* **2016**, *37*, 506–541.
- (54) Fernandez Galván, I.; Vacher, M.; Alavi, A.; Angeli, C.; Autschbach, J.; Bao, J. J.; Bokarev, S. I.; Bogdanov, N. A.; Carlson, R. K.; Chibotaru, L. F.; et al., OpenMolcas: From Source Code to Insight. 2019; https://chemrxiv.org/articles/OpenMolcas_From_Source_Code_to_Insight/8234021/1.
- (55) Lee, C.; Yang, W.; Parr, R. G. Development of the Colle-Salvetti correlation-energy formula into a functional of the electron density. *Phys. Rev. B* **1988**, *37*, 785.
- (56) Becke, A. D. Density-functional thermochemistry. III. The role of exact exchange. *J. Chem. Phys.* **1993**, *98*, 5648–5652.
- (57) Becke, A. D. A new mixing of Hartree–Fock and local density-functional theories. *J. Chem. Phys.* **1993**, *98*, 1372–1377.

- (58) Grimme, S.; Antony, J.; Ehrlich, S.; Krieg, H. A consistent and accurate ab initio parametrization of density functional dispersion correction (DFT-D) for the 94 elements H-Pu. *J. Chem. Phys.* **2010**, *132*, 154104.
- (59) Grimme, S. Semiempirical GGA-type density functional constructed with a long-range dispersion correction. *J. Comput. Chem.* **2006**, *27*, 1787–1799.
- (60) Rimola, A.; Taquet, V.; Ugliengo, P.; Balucani, N.; Ceccarelli, C. Combined quantum chemical and modeling study of CO hydrogenation on water ice. *Astron. Astrophys.* **2014**, *572*, A70.
- (61) McQuarrie, D. *Statistical Mechanics*; New York: Harper and Row, 1976.
- (62) Boys, S. F.; Bernardi, F. d. The calculation of small molecular interactions by the differences of separate total energies. Some procedures with reduced errors. *Mol. Phys.* **1970**, *19*, 553–566.
- (63) Wakelam, V.; Loison, J.-C.; Mereau, R.; Ruaud, M. Binding energies: new values and impact on the efficiency of chemical desorption. *Mol. Astrophys.* **2017**, *6*, 22–35.
- (64) Sameera, W. M. C.; Senevirathne, B.; Andersson, S.; Maseras, F.; Nyman, G. ONIOM(QM:AMOEBA09) Study on Binding Energies and Binding Preference of OH, HCO, and CH₃ Radicals on Hexagonal Water Ice (Ih). *J. Phys. Chem. C.* **2017**, *121*, 15223–15232.
- (65) Codella, C. et al. Seeds of Life in Space (SOLIS). II. Formamide in protostellar shocks: Evidence for gas-phase formation. *Astron. Astrophys.* **2017**, *605*, L3.
- (66) Barone, V.; Latouche, C.; Skouteris, D.; Vazart, F.; Balucani, N.; Ceccarelli, C.; Lefloch, B. Gas-phase formation of the prebiotic molecule formamide: insights from new quantum computations. *Mon. Not. R. Astron. Soc.* **2015**, *453*, L31–L35.

- (67) Skouteris, D.; Vazart, F.; Ceccarelli, C.; Balucani, N.; Puzzarini, C.; Barone, V. New quantum chemical computations of formamide deuteration support gas-phase formation of this prebiotic molecule. *Mon. Not. R. Astron. Soc.* **2017**, *468*, L1–L5.

For TOC Only

